# PHOTOFOCUSING OF MICROORGANISMS SWIMMING IN A FLOW WITH SHEAR

R. J. CLARKE[1]

## Abstract

Some swimming microorganisms are sensitive to light, and this can affect the way in which they negotiate their environment. In particular, photophobic cells are repelled from unfavourable light conditions, and in a quiescent fluid environment this can be observed as elevated cell levels in regions away from these light conditions. This photoresponsive effect is of interest due to its potential technological applications. For example, the use of light to focus and direct cells could be used as a convenient means to separate out the algae used in biofuel production (for example, hydrogen), or exploited within devices for biodetection of environmental contaminants. However, in these types of situations the swimming cells will usually be suspended in a flow with shear. In this environment, it has previously been shown that cells can become hydrodynamically trapped in regions of high fluid shear, and so the extent to which photofocusing can occur under these conditions is not immediately clear. Moreover, in applications where the light must pass through appreciable volumes of the suspension, cells will typically absorb light and so shade each other from the illumination. As such, the intensity at any point in the flow is dependent upon the global cell concentration. Hence, in this study we model the coupled influence of fluid shear and cell photosensitivity on a suspension of swimming microorganisms, and ask under what circumstances a suspension of photophobic cells might be focused into high concentration regions.

## 1. Introduction

Microorganisms are subject to many of the same survival pressures experienced by larger animals, for example, the need to fuel themselves and avoid predators. For this reason, many microorganisms that live in a fluid environment, swim and can adjust their swimming in response to a number of different environmental stimuli. Common examples include responses to chemical gradients (*chemotaxis*) [1, 2], gradients in fluid shear (*rheotaxis*) [20] and gravitational acceleration (*gravitaxis*) [14]. One way

---

[1]Department of Engineering Science, University of Auckland, New Zealand;
e-mail: rj.clarke@auckland.ac.nz.

in which a microorganism can swim up gravitational potentials is by possessing a centre-of-mass which is different from its geometric centre. The requirement that the cells experience no net torque (due to the lack of inertia at the microscopic scales) means that cells rotate until the centre-of-mass and geometric centre are aligned with the direction of gravitational acceleration. If there is a background flow that induces an additional hydrodynamic torque on the cell, the zero-torque orientation will be offset from the direction of gravity. This bias in swimming direction due to a balance of viscous and gravitational torques is referred to as *gyrotaxis*, and can lead to effects such as hydrodynamic focusing [14]. In microorganism suspensions containing large numbers of individuals, these responses can lead to large-scale spatial and temporal changes in the bulk density of cells. In situations where there is an upwards swimming bias (either due to gravity or vertical gradients in oxygen, say), this can lead to an unstable density stratification (since the cells are generally slightly denser than the surrounding water), leading to the onset of bulk convection of both cells and fluid [3].

The response that we concentrate on here is cell sensitivity to light (photo-sensitivity). This is an effect often associated with photosynthetic algae, however, many different types of bacteria are also photosensitive. One of the first observations of bacterial phototaxis was made in 1881 by Ehrenberg [4]. He noted that a species of purple sulphur bacterium accumulated at a bright spot of light on an otherwise unilluminated slide. He further observed that these bacteria were attracted to specific wavelengths of light, some outside of the visible spectrum, and also wavelengths in the yellow-green part of the spectrum.

The review of photosensory behaviour in bacteria by Hader [9] suggests three different categories of light sensitivity: (i) phototaxis, where cells orientate in response to favourable light conditions (in analogy to chemotaxis, where cells orient in response to nutrient sources), (ii) photokinesis, where cells increase or decrease their speeds in response to local light levels and (iii) photophobia, where cells reverse their swimming direction in response to abrupt changes in light conditions. The reversal can be achieved in a number of ways, including for bacteria such as *Rhodospirillum rubrum*, reversal of the direction of flagella rotation. Other microorganisms, such as *Halobacterium* have flagellum (-a) at both ends of their cell bodies, and can reverse swimming directions by switching the flagellum (-a) being rotated. Photophobia can lead to trapping of cells in localized dark or bright spots, depending upon whether the photophobic cells are repelled by an increase (step-up photophobia) or decrease (step-down photophobia) in light levels. Whereas phototaxis depends upon light gradients, both photokinesis and photophobia are functions of the pointwise light conditions.

The bulk response of cells that align with light gradients (phototactic) has previously been modelled, notably by Vincent and Hill [17], and Williams and Bees [18], and examined in the context of bulk suspension motions such as bioconvection [6, 7, 12]. These models incorporate the effects of light absorption and scattering by other cells in the suspension, and predict cell-rich layers at finite depth where light levels are sufficiently high to meet the cells' needs, but not so high as to be damaging. In these studies, the bulk density of cells is typically modelled

using an advection–diffusion equation, which describes the density of cells at each location as a function of time [15]. The diffusivity comes from inherent randomness in cell swimming, and is due more to biological variability rather than Brownian effects (which are considered to be much smaller in magnitude). Traditionally, the coefficient of diffusivity has been modelled as being proportional to the variance in swimming direction, however, more recent theoretical descriptions have approached it from the perspective of generalized Taylor dispersion theory [1, 11]. Advection of cells is due to their own motility, as well as by the background flow. The orientation of each cell is stochastic, and determined by an orientation probability distribution that satisfies the Fokker–Planck equation [14].

However, in the presence of a nonhomogeneous background flow shear, this decoupling of cell density from cell orientation does not capture certain phenomena, such as the interplay between cell geometry and fluid shear. Such effects can be reproduced by a higher-dimensional Smoluchowski equation, which considers the density of cells at each point with a particular swimming orientation [16]. Using such a model, Bearon and Hazel [2] have shown that nonspherical cells can become trapped in regions of high fluid shear.

In this study, we therefore combine the Smoluchowski model for describing suspensions of photophobic swimming cells within a background shear flow. This allows us to investigate whether such cells can focus under different background shear conditions, and we concentrate here on nonbottom heavy, nonspherical cells (for example, purple sulphur bacteria which have significant ecological impact upon the bodies of water in which they are found). Here the interplay between cell geometry and flow shear can be expected to be the most pronounced. We consider the semi-dilute regime, where the influence of the cells upon the hydrodynamics, which can be captured through the inclusion of a bacterial stress in the flow equations, is small compared to the magnitude of the background flows. We do suppose, however, that the suspension is still sufficiently dense for cell shading effects to be important. For more concentrate suspensions, however, these cell hydrodynamics can be significant, and require explicit inclusion of the swimmers in the hydrodynamics. Examples include the Stokesian dynamics simulations of squirmers by Ishikawa and Pedley [10], who undertake full boundary element method (BEM) computations of a swimmer suspension, and also Wioland et al. [19] who use singularity (diplole) representations for the swimmers.

The interest of this interplay is partly motivated by the recent experiments of Garcia et al. [5], who demonstrated focusing of phototactic cells suspended in flow through a circular pipe. In these experiments, light was directed down the length of the pipe, and so the effect is analogous to the gyrotactic focusing described by Pedley and Kessler [14]. However, we instead model here the situation of a source of light that is directed perpendicular to the flow of cell suspensions through a channel (see Figure 1 for an illustration) which is perhaps more practical in applications such as microbe detection sensors. We ask whether similar focusing can occur when the cells are photophobic, but not phototactic.
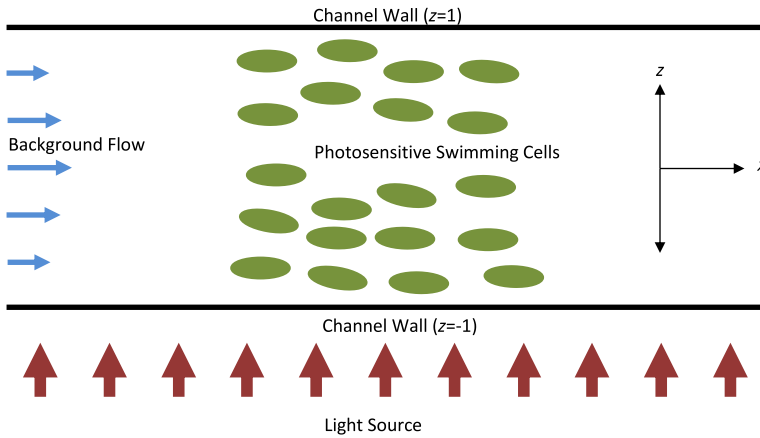
FIGURE 1. A schematic of the geometry, showing swimming light-sensitive cells suspended in fluid flowing through a two-dimensional channel. A uniform source of light illuminates the channel from below.

## 2. Formulation

We consider the steady dynamics of a suspension of swimming microorganisms contained between two solid surfaces located at $z^* = \pm W/2$. For simplicity we assume that the suspension is uniform in the horizontal directions, $x$ and $y$. Cell transport is modelled using the Smoluchowski equation, which describes the density of cells $\psi(x, p)$ having orientation $p$ at a given location $x$ [16]. We suppose that the effects of gravity are not considered here (asterisks denote dimensional quantities):

$$(u^* + V^*(I^*)p) \cdot \nabla_x^* \psi^* - D\nabla_x^{*2}\psi^* - d_r \nabla_p^2 \psi^* + \nabla_p \cdot [\dot{p}\psi^*] = 0, \tag{2.1}$$

with

$$\dot{p} = \beta p \cdot E^* \cdot (I_d - pp) + \tfrac{1}{2}\omega^* \cdot (p \times \nabla_p), \tag{2.2}$$

where $D$ and $d_r$ are translational and rotational diffusivities which capture biological variability rather than (much smaller) Brownian effects, $I_d$ is the identity matrix and $E^* = (\nabla u^* + \nabla u^{*T})/2$ is the rate of strain of the flow $u^*$. The shape parameter $\beta$ is given by Pedley and Kessler [14], and is zero for spherical cells and unity for rod-shaped cells. The background flow is represented by $u^*$, with associated vorticity $\omega^*$. Here $\nabla_x^*$ and $\nabla_p$ represent derivatives in Cartesian space and orientation space, respectively.

We consider here a photophotobic response, where the cells reverse their swimming direction when they encounter light about some threshold value $I_c$. If we suppose that the light intensity is sufficiently close to this threshold throughout the fluid, we can expand swimming speed about $I_c$ and the simplest phenomelogical model which captures this response is given by the following relationship between swimming velocity and light intensity:

$$V^*(I^*)p = -\xi(I^* - I_c)p,$$

where $V_0 = \xi I_c$ is the swimming speed in the absence of any illumination.

Assuming that the source of the light is from directly below, its intensity is modelled using the Lambert–Beer law [18], which models the absorption of light by the cells in the suspension

$$I^*(\boldsymbol{x}) = I_s \exp\left(-\alpha \int_{-1}^{z} n^*(x, y, z') \, dz'\right),\tag{2.3}$$

where $I_s$ represents the strength of the light source at the bottom of the channel ($z = -1$) and $\alpha$ is the cell's light absorption coefficient.

The cell concentration is given by

$$n^*(\boldsymbol{x}) = \int \psi^* \, d\boldsymbol{p}.$$

Under the following nondimensionalization

$$\boldsymbol{x}^* = (W/2)\boldsymbol{x}, \quad t^* = (1/d_r)t, \quad \boldsymbol{u}^* = U\boldsymbol{u}, \quad V^* = V_0 V, \quad I^* = I_s I, \quad \psi^* = N\psi,$$

where $U$ is the maximum flow speed and $N$ is the total number of cells per cross-sectional area (constant $x$ plane), we obtain (2.1)–(2.3) in the following form:

$$(Pe\boldsymbol{u} + \epsilon V(I)\boldsymbol{p}) \cdot \boldsymbol{\nabla}_x \psi - \epsilon^2 d\nabla_x^2 \psi$$
$$+ \beta Pe \boldsymbol{\nabla}_p \cdot (\boldsymbol{p} \cdot \boldsymbol{E} \cdot (\boldsymbol{I}_d - \boldsymbol{pp}))\psi + \frac{Pe}{2}\boldsymbol{\omega} \cdot (\boldsymbol{p} \times \boldsymbol{\nabla}_p \psi) - \nabla_p^2 \psi = 0,\tag{2.4}$$

and

$$I(\boldsymbol{x}) = \exp\left(-\kappa \int_{-1}^{z} \left(\int \psi(x, y, z', \boldsymbol{p}) \, d\boldsymbol{p}\right) dz'\right)\tag{2.5}$$

with

$$Pe = 2U/Wd_r, \quad d = Dd_r/V^2, \quad \epsilon = 2V/Wd_r, \quad \chi = I_s/I_c, \quad \kappa = \alpha W/2.$$

Following Bearon and Hazel [2] and considering the particular case of Poiseuille flow through a two-dimensional (2D) channel in the $x - z$ plane, we have $\boldsymbol{u} = (1 - z^2, 0)$. We further assume that cell orientations are also confined to this plane, and in this setting the cell orientations can be parameterized as $\boldsymbol{p} = (\cos\theta, \sin\theta)$ for $0 \le \theta < 2\pi$ (with $\theta = 0$ corresponding to the positive $x$-axis). Seeking steady cell populations that are fully developed in the streamwise direction (that is, $\psi(x, z, \theta, t) = \psi(z, \theta)$), (2.4)–(2.5) take the form

$$\epsilon \frac{\partial}{\partial z}\left(\sin\theta V(I)\psi - \epsilon d\frac{\partial\psi}{\partial z}\right) + \frac{\partial}{\partial\theta}\left(zPe(1 - \beta\cos(2\theta))\psi - \frac{\partial\psi}{\partial\theta}\right) = 0,\tag{2.6}$$

and

$$I(z) = \exp\left(-\kappa \int_{z}^{1}\left(\int_{0}^{2\pi} \psi(z', \theta) \, d\theta\right) dz'\right).\tag{2.7}$$

These are subject to no-flux boundary conditions

$$\int\left(\sin\theta V(I) - \epsilon d\frac{\partial\psi}{\partial z}\right)\bigg|_{z=\pm 1} d\theta = 0,$$

which as Bearon and Hazel [2] have shown, can be replaced with the stronger condition

$$\left(\sin\theta V(I) - \epsilon d\frac{\partial\psi}{\partial z}\right)\bigg|_{z=\pm 1} = 0. \tag{2.8}$$

In addition, we have the normalization condition

$$\int_{-1}^{1}\int_{0}^{2\pi}\psi(z,\theta)\,d\theta\,dz = 1.$$

The nondimensional relationship between swimming speed and light then takes the form

$$V(I) = 1 - \chi I,$$

where $\chi = I_s/I_c$.

## 3. Numerical implementation

We solve the governing equations using a finite-element approach. By multiplying through by global weighting functions $N(\theta, z)$ and integrating over $(\theta, z)$ space and then integrating by parts with respect to $z$, a weak form of the Smoluchowski equation (2.6) can be obtained

$$\int_{-1}^{1}\int_{0}^{2\pi}\left\{\epsilon\frac{\partial N}{\partial z}\left(\sin\theta V(I)\psi - \epsilon d\frac{\partial\psi}{\partial z}\right) + N\frac{\partial}{\partial\theta}\left(zPe(1-\beta\cos(2\theta))\psi - \frac{\partial\psi}{\partial\theta}\right)d\theta\,dz\right\} = 0, \tag{3.1}$$

where we have used the zero flux condition (2.8). We decompose the domain into $M$ elements, and express the density $\psi$ and illumination $I$ in terms of quadratic basis functions defined on each element as

$$\psi(\theta, z) = \sum_{i=1}^{3}\sum_{j=1}^{3}\Psi_{ij}\phi_{ij}, \quad I(z) = \sum_{i=1}^{3}I_i\psi_i,$$

where

$$\psi_1 = 2(\xi-1)(\xi-0.5), \quad \psi_2 = 4\xi(1-\xi), \quad \psi_3 = 2\xi(\xi-0.5), \quad \phi_{ij} = \psi_i\psi_j$$

for $0 < \xi < 1$. Then making the Galerkin assumption $N = \psi_j$, we can express (3.1) and (2.7) as the nonlinear system of equations

$$\mathcal{F}(\mathbf{\Psi}, \mathbf{I}) = 0, \quad \mathbf{I} = \mathcal{G}(\mathbf{\Psi}),$$

respectively, where $\mathbf{I}$ and $\mathbf{\Psi}$ hold the nodal values of $I$ and $\psi$, respectively. The implementation of this numerical scheme was implemented in Matlab, and solved using *fsolve* (with the Jacobian provided explicitly, to reduce the number of function evaluations required each iteration). Converged results were obtained using 60 elements in the $z$- and $\theta$-directions.

TABLE 1. Reference table for the different cases considered. The degree of light absorption by the cells is measured by $\kappa$, and the strength of the background flow by $Pe$.

| Figure | $Pe$ | $\kappa$ |
|--------|------|----------|
| 2 | 1 | 0.1 |
| 3 | 1 | 0.5 |
| 4 | 1 | 0.9 |
| 5 | 5 | 0.1 |
| 6 | 5 | 0.5 |
| 7 | 5 | 0.9 |

## 4. Results

In what follows, we present the cell densities and light intensities for a range of different possible light sensitivities ($\chi$), and we consider cells with a rod-like shape characteristic of many bacteria ($\beta = 0.9$) and assume $D = 0.01$. A list of the different cases being considered is given in Table 1.

In Figure 2 we consider the case where cell absorption is relatively weak ($\kappa = 0.1$) and the background flow is moderate ($Pe = 1$). When the cells are completely insensitive to light levels ($\chi = 0$), we see that the cell distribution is largely uniform across the width of the channel, except for thin regions near the channel walls where diffusion must counteract advection in order for the no-flux condition to be satisfied. The light intensity can be seen to drop off linearly by about 50% across the width of the channel. When we then consider the case where the cells are light sensitive with $\chi = 1$, we see an increase in the concentration of cells at the side of the channel closest to the light source, that is, $z = -1$. This can be explained by the fact that the magnitude of the swimming velocity is at its minimum when $I = 1$, as shown in the right-hand column. When the sensitivity is increased to $\chi = 2$ we see (a less pronounced) elevated cell concentrations shift towards $z \approx 0.8$, due the fact that the minimum in the magnitude of speed now occurs on this side of the channel. As the sensitivity increases to $\chi = 3$, we see that there remains a slight elevation in cell density towards the upper wall ($z = 1$), however, this is less marked than for $\chi = 2$, due to the fact that the variation in swimming speeds is more pronounced for that level of light sensitivity, that is, compare a 15% variation in swimming speed when $\chi = 2$, to a 5% variation when $\chi = 3$.

When the light absorption of the cells is increased to $\kappa = 0.5$, we observe some important differences. In Figure 3 we again note a shift of cell towards the source of the light at $z = -1$ when $\chi = 1$, and this is more localized than that observed when $\kappa = 0.1$. The differences are even more stark when light sensitivity is increased to $\chi = 2$. We note a reversal in swimming direction at $z \approx 0.8$, which leads to a localized peak in the cell density profile, that is, cell focusing, at the same point in the channel. As cell light sensitivity is increased still further to $\chi = 3$, the minimum swimming speed shifts to the upper channel wall ($z = 1$), which also leads to a cell density bias towards the upper wall but no longer a well-defined peak in cell concentration.
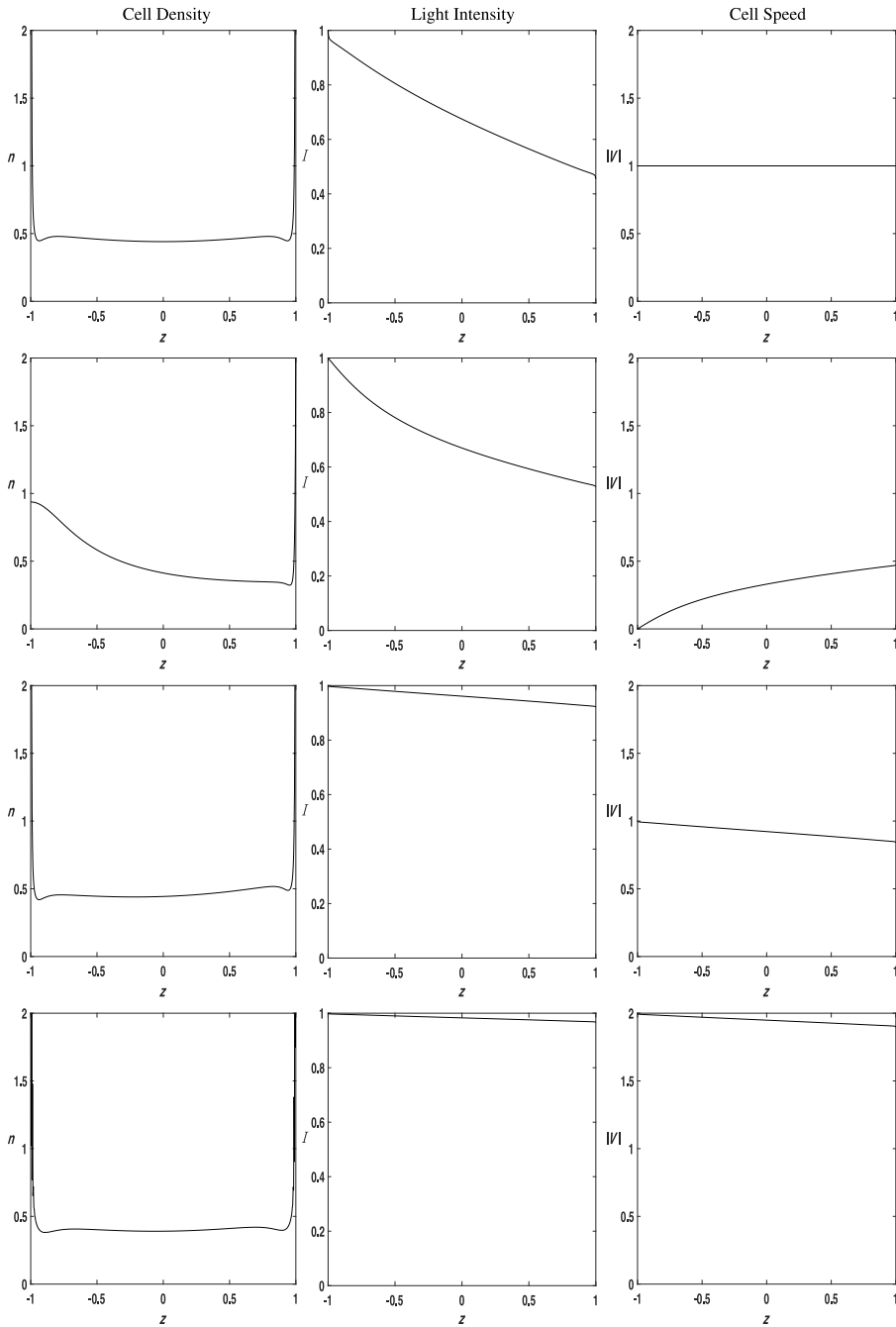
FIGURE 2. *Weakest flow* ($Pe = 1$), *weakest absorption* ($\kappa = 0.1$): (left column) cell density, (middle column) light intensity and (right column) swimming speed and with photosensitivity (first row) $\chi = 0$, (second row) $\chi = 1$, (third row) $\chi = 2$, (fourth row) $\chi = 3$.
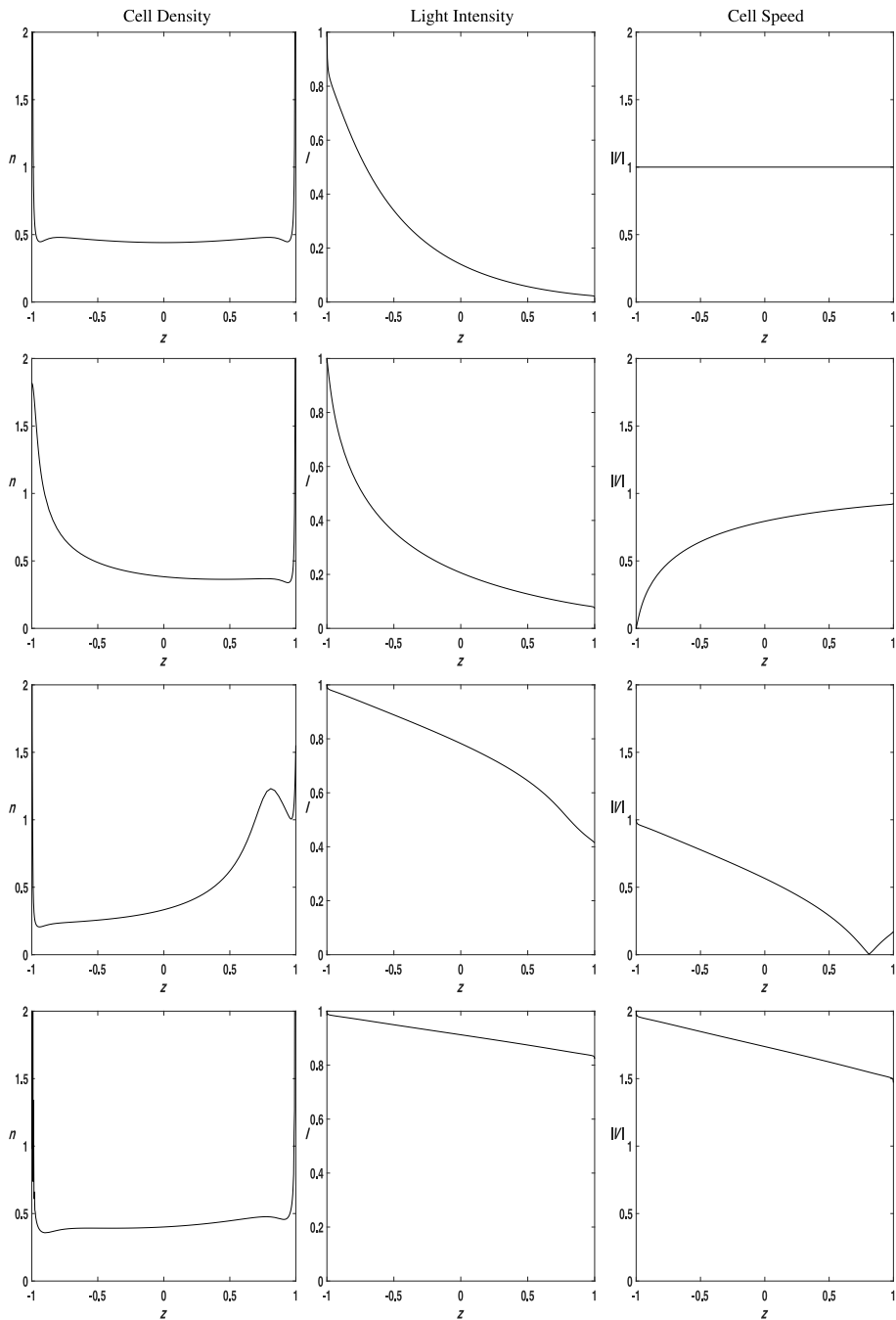
FIGURE 3. *Weakest flow* (*Pe* = 1), *intermediate absorption* (*κ* = 0.5): (left column) cell density, (middle column) light intensity and (far right column) swimming speed and with photosensitivity (first row) $\chi = 0$, (second row) $\chi = 1$, (third row) $\chi = 2$, (fourth row) $\chi = 3$.
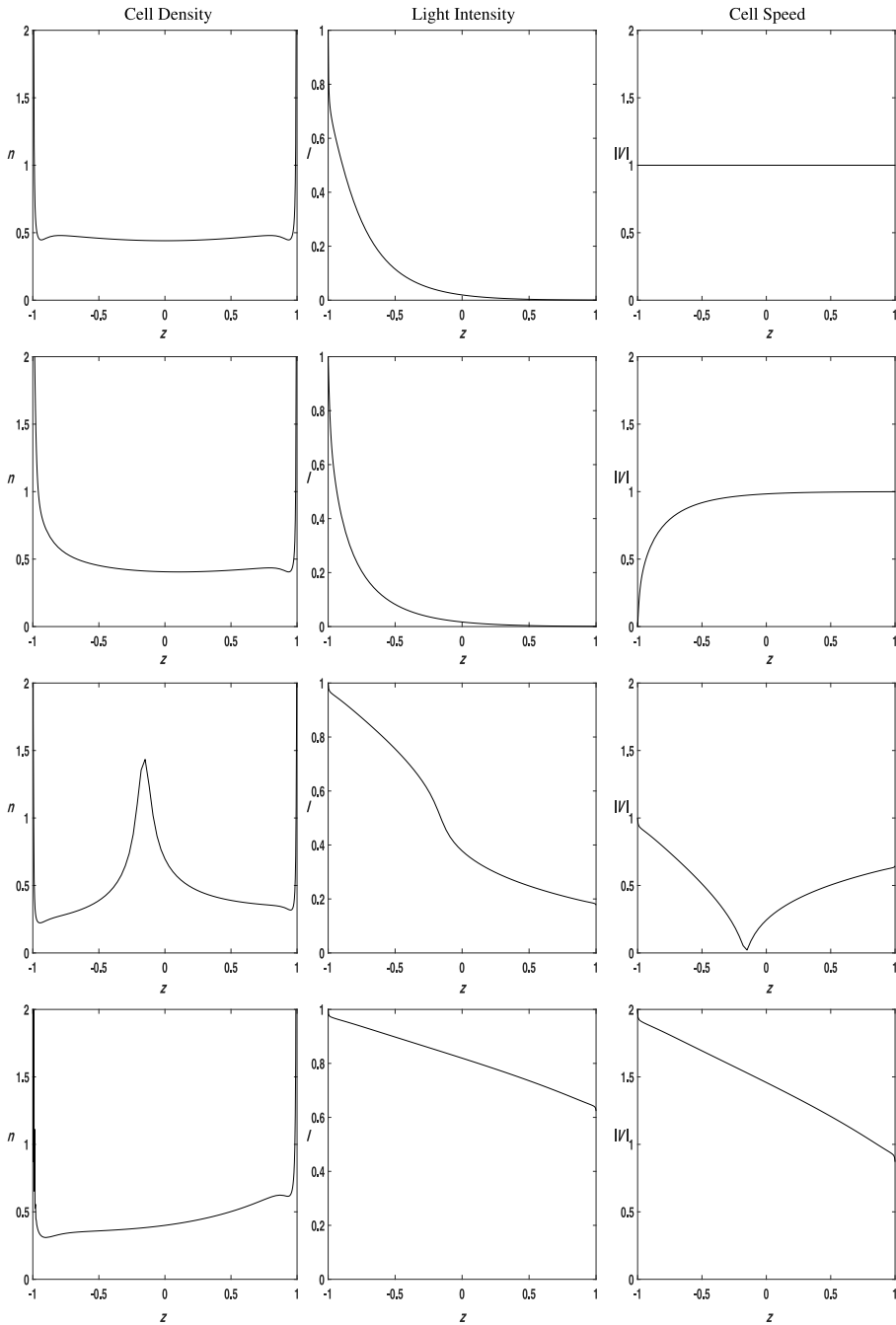
FIGURE 4. *Weakest flow* ($Pe = 1$), *strongest absorption* ($\kappa = 1$): (left column) cell density, (middle column) light intensity and (far right column) swimming speed and with photosensitivity (first row) $\chi = 0$, (second row) $\chi = 1$, (third row) $\chi = 2$, (fourth row) $\chi = 3$.

As the ability of cells to absorb light increases still further ($\kappa = 1$, Figure 4), for $\chi = 2$ we again see a reversal of swimming direction, but now closer to the light source, at $z \approx -0.2$. As before, this is associated with cell focusing.

If we further increase the strength of the background flow, such that $Pe = 5$, we start to see in Figure 5 an increase in the number of cells either side of the centre of the channel, as previously reported by Bearon and Hazel [2] for nonphotosensitive cells (albeit at smaller value of diffusivity, $d$), which they referred to as *hydrodynamic trapping*. As the cells become more light sensitive, we see a shift in profile towards the light source, followed by a shift towards the upper wall as sensitivity is increased still further.

At lower flow rates, when the cell absorption is increased to $\kappa = 0.5$ we see the onset of cell photofocusing for $\chi = 2$ (Figure 6). Under these flow conditions we see that the cell peak has shifted towards the centre of the channel, whereas when $Pe = 1$ the peak was far closer to the upper wall. This suggests some coupling between the flow shear and phototaxis. We also see that there is still no photofocusing visible for the cells with the greatest light sensitivity ($\chi = 3$), although there is greater bias in cell densities towards the upper wall than observed at the lower flow rates.

When the light absorption is greatest, in Figure 7, we do observe a reappearance of cell photofocusing at $\chi = 3$ close to the upper channel wall, which disappears under the more moderate background flow conditions. This is in addition to the cell focusing at $\chi = 2$, with the peak now closer to the light source than for the case where $\kappa = 0.5$. In both cases, the sharpness of the peak is relatively low, and arguably does not provide a high-quality photofocusing effect.

## 5. Conclusions

In this study, we examined how photophobic swimming microorganisms are distributed within a flow through a two-dimensional channel, and asked whether photofocusing can occur in the presence of a background flow. Their response to light was modelled using a simple phenomenological model whereby cells slow, and then reverse their swimming direction at some critical light intensity. The transport of cells was described using a Smoluchowski equation, rather than the lower-dimensional cell conservation equations used in some previous photosensitive cell models, as the former better captures effects such as hydrodynamic trapping [2].

We observe in the case studies considered here that the interplay between background flow and photophobia does appear to be important. The photophobic response, which is perpendicular to the direction of flow due to the direction of the illumination, is seen to lead to different cell density profiles that are observed in the absence of light. One likely explanation is that the photophobic response causes the cells to migrate into regions of the channel where there are different levels of flow shear, which in turn affect the bulk transport of the cells. We have seen that under moderate levels of light absorption by the cells, a photofocused peak of high density cells can be attained. We note also that increasing absorption tends to bring the peak
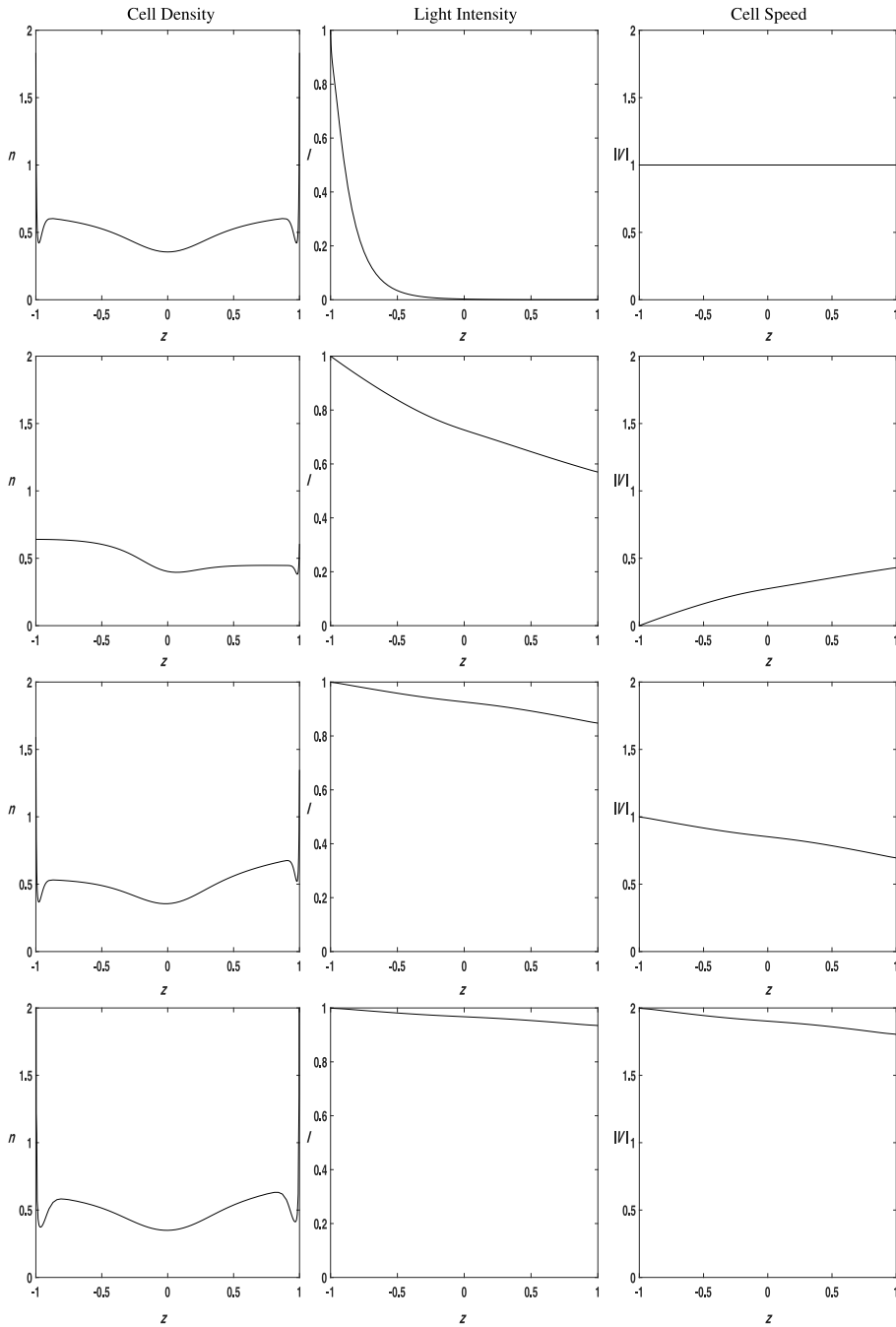
FIGURE 5. *Strongest flow* ($Pe = 5$), *weakest absorption* ($\kappa = 0.1$): (left column) cell density, (middle column) light intensity and (right column) swimming speed and with photosensitivity (first row) $\chi = 0$, (second row) $\chi = 1$, (third row) $\chi = 2$, (fourth row) $\chi = 3$.
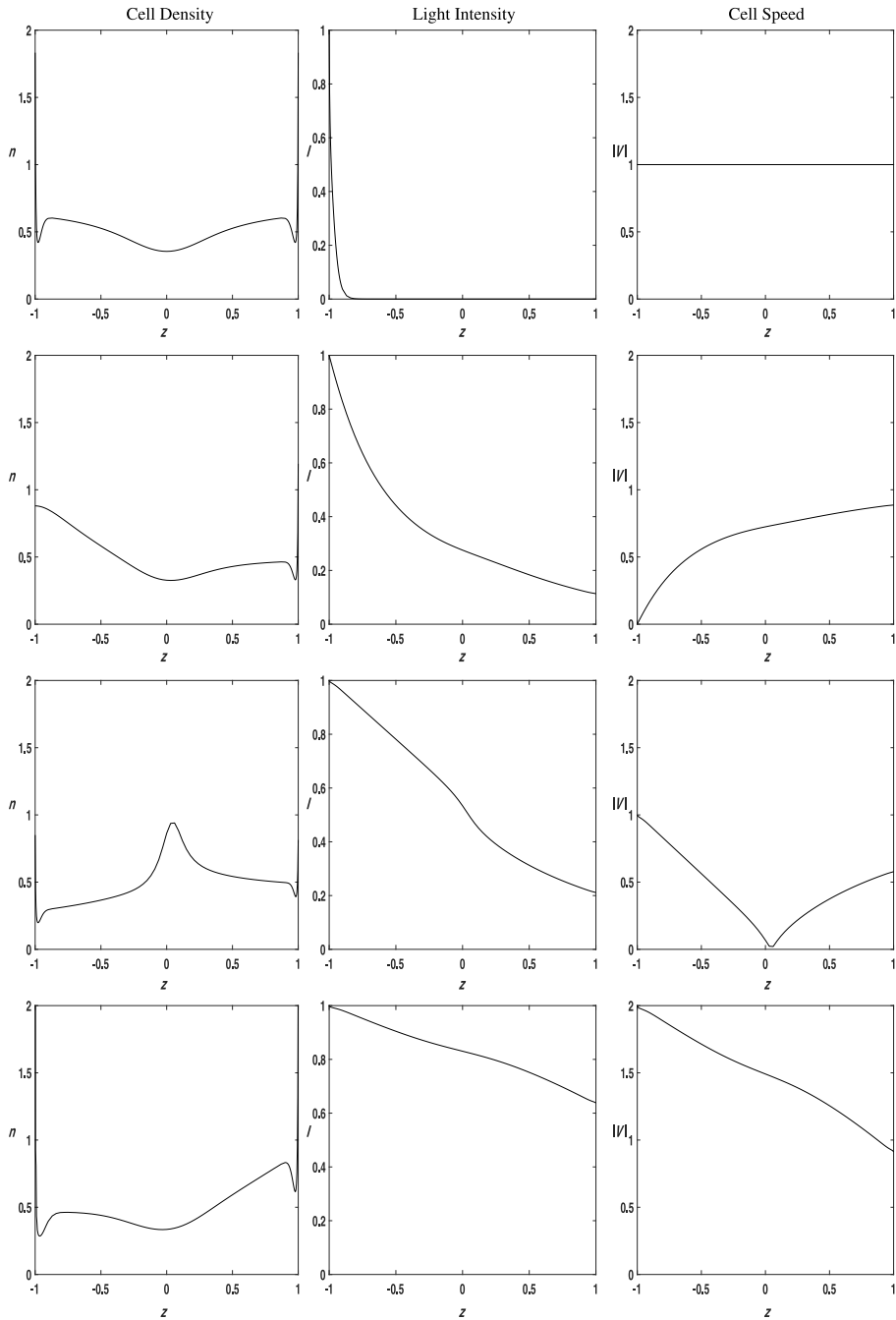
FIGURE 6. *Strongest flow* (*Pe* = 5), *intermediate absorption* ($\kappa$ = 0.5): (left column) cell density, (middle column) light intensity and (right column) swimming speed and with photosensitivity (first row) $\chi = 0$, (second row) $\chi = 1$, (third row) $\chi = 2$, (fourth row) $\chi = 3$.
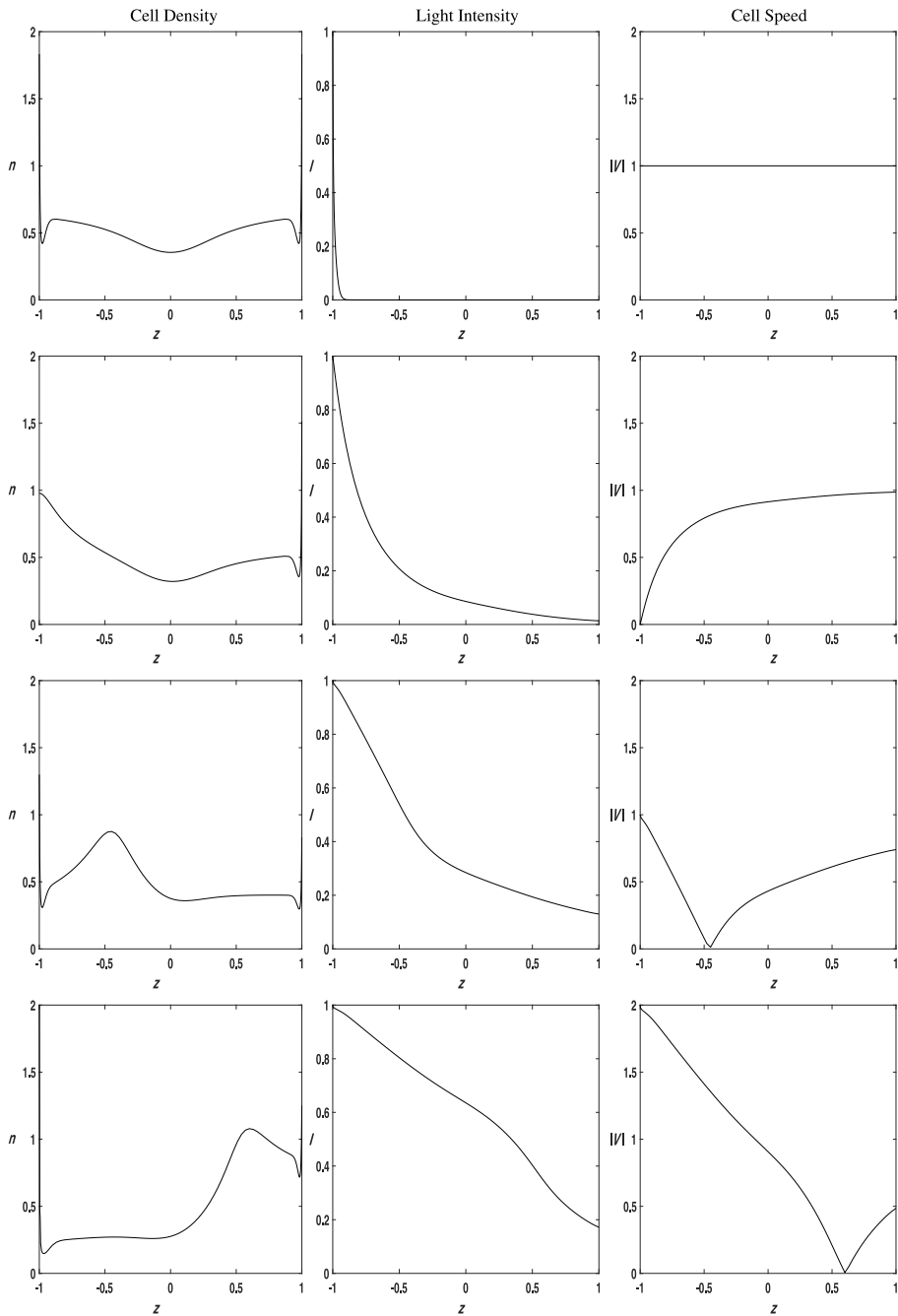
FIGURE 7. *Strongest flow* (*Pe* = 5), *strongest absorption* (*κ* = 1): (left column) cell density, (middle column) light intensity and (right column) swimming speed and with photosensitivity (first row) *χ* = 0, (second row) *χ* = 1, (third row) *χ* = 2, (fourth row) *χ* = 3.

closer to the light source and sharpen the peak, provided that the background flow shear is not too high. It would appear, however, that quality (sharpness) of any photofocused peak does degrade as the strength of the background flow is increased. The shift in the location of the peak under these stronger flows appears to be more involved. In weak flow it appears to move towards the upper channel wall (away from the light source), whereas in stronger flow it is located quite centrally within the channel. Also, it is worth noting that the hydrodynamic trapping reported by Bearon and Hazel [2] is still present under the stronger flows ($Pe = 5$) when cell absorption is weak, though it seems to be degraded at greater levels of cell absorption. And so in terms of photofocusing applications, these findings suggest that photofocusing in the presence of a background flow shear is possible, provided the cells' photophobic response (as characterized by $\chi$ here) is not too weak or strong. There is also some suggestion that the peak can be moved closer to the light source by increasing the strength of the background flow, however, this also seems to degrade the sharpness of the peak.

We have concentrated here on photophobic microorganisms, however, as mentioned in the introduction, some photosensitive microorganisms are phototactic, meaning that they orientate along favourable light gradients. Models which incorporate such biases in swimming directions must acknowledge that the cells experience no net force (since there is no inertia at these lengthscales). One way in which this can be achieved is by incorporating a phototactic torque into the kinematic equation (2.2). In previous studies that have used the cell conservation approach, this torque has been taken to depend on light indirectly, through a cell centre-of-mass which depends upon light intensity, or a (photoreactive) torque that depends directly upon light intensity [18]. Both of these models of phototaxis could be applied to the more general Smoluchowski model presented here.

Something else that we have not considered in this study is the fact that cells can scatter light, as well as absorb it. These effects can be modelled by replacing the Lambert–Beer law (2.5) with an integro-differential equation that captures changes in light intensity along a ray through both absorption and/or isotropic scattering [8, 13], or anistropic scattering [7]. It would be an interesting extension to the model presented here to include such effects, to determine their influence upon cell densities within a suspension, and the likelihood of photofocusing being achieved.

We have also focused here on microorganisms with the characteristics of bacteria, for instance, having a rod-like shape. In many applications, however, the photosensitive microorganisms of interest are algae, which can be less elongated. Another important difference is that algae can be bottom-heavy, meaning that they experience a gyrotactic torque. These two physiological differences could be included in this model by changing the value of $\beta$ and including a gyrotactic torque into the kinematic equation (2.2), respectively (although there may be some low gravity regimes, such as closed-loop spacecraft life-support systems, where the findings of this study might also apply for bottom-heavy microorganisms). It is also worth mentioning that the background flow itself can be influenced by the presence of cells, leading to an additional stress term, sometimes referred to as the *bacterial stress* (especially

when the swimmers are propelled from behind, for example, by a flagellum). This accounts for the fact that cells do not deform in the same way as the volume of fluid that they have displaced. We have assumed in this study that the background flow shear is sufficiently strong so as to dominate any additional flows generated by these bacterial stresses, although it could be of interest to include these effects for the case of weaker background flows. Another obvious extension of this study would be to examine the influence of photosensitivity in three-dimensional regimes. Finally, the correct physical boundary conditions remains an open problem in the Smoluchowski description of cell transport. The no-flux condition does not fully recognize the fact that the cell orientations may be influenced by hydrodynamic interaction with the channel walls, and incorporating these considerations into models of biologically active matter is the subject of wider on-going research.

## Acknowledgements

## References

[1]  R. N. Bearon, "An extension of generalized Taylor dispersion in unbounded homogeneous shear flows to run-and-tumble chemotactic bacteria", *Phys. Fluids* **15**(6) (2003) 1552–1563; doi:10.1063/1.1569482.

[2]  R. N. Bearon and A. L. Hazel, "The trapping in high-shear regions of slender bacteria undergoing chemotaxis in a channel", *J. Fluid Mech.* **771** (2015) 1–13; doi:10.1017/jfm.2015.198.

[3]  M. A. Bees and N. A. Hill, "Linear bioconvection in a suspension of randomly-swimming, gyrotactic micro-organisms", *Phys. Fluids* **10** (1995) 1864; doi:10.1063/1.869704.

[4]  T. W. Ehrenberg, "Bakterium photometricum. Ein Beitrag zur vergleichenden Physiologie des Licht-und Farbensinnes Pfluegers", *Arch Gesamte Physiol Menschen Tiere* **42** (1883) 183–186.

[5]  X. Garcia, S. Rafai and P. Peyla, "Light control of the flow of phototactic microswimmer suspensions", *Phys. Rev. Lett.* **110** (2013) 138106; doi:10.1103/PhysRevLett.110.138106.

[6]  S. Ghorai and N. A. Hill, "Penetrative phototactive bioconvection", *Phys. Fluids* **17** (2005) 074101; doi:10.1063/1.1947807.

[7]  S. Ghorai and M. K. Panda, "Bioconvection in an anistropic scattering suspension of phototactic algae", *Eur. J. Mech. (B/Fluids)* **41** (2013) 81–93; doi:10.1016/j.euromechflu.2012.07.001.

[8]  S. Ghorai, M. K. Panda and N. A. Hill, "Bioconvection in a suspension of isotropically scattering phototactic algae", *Phys. Fluids* **22** (2010) 071901; doi:10.1063/1.3457163.

[9]  D. P. Hader, "Photosensory behavior in procaryotes", *Microbiol. Rev.* **51** (1987) 1–21; https://www.ncbi.nlm.nih.gov/pmc/articles/PMC373089/.

[10]  T. Ishikawa and T. J. Pedley, "Coherent structures in monolayers of swimming particles", *Phys. Rev. Lett.* **100** (2009) 088103; doi:10.1103/PhysRevLett.100.088103.

[11]  A. Manela and L. Frankel, "Generalized Taylor dispersion in suspensions of gyrotactic swimming micro-organisms", *J. Fluid Mech.* **490** (2003) 99–127; doi:10.1017/S0022112003005147.

[12]  M. K. Panda and S. Ghorai, "Penetrative phototactic bioconvection in a two-dimensional non-scattering suspension", *Phys. Fluids* **28** (2016) 054105; doi:10.1063/1.4948543.

[13]   M. K. Panda and S. Ghorai, "Penetrative phototactic bioconvection in an isotropic scattering suspension", *Phys. Fluids* **25** (2013) 071902; doi:10.1063/1.4813402.

[14]   T. J. Pedley and J. O. Kessler, "Hydrodynamic phenomena in suspensions of swimming microorganisms", *Annu. Rev. Fluid Mech.* **24** (1992) 313–358; doi:10.1146/annurev.fl.24.010192.001525.

[15]   T. J. Pedley and J. O. Kessler, "A new continuum model for suspensions of gyrotactic micro-organisms", *J. Fluid. Mech.* **212** (1990) 155–182; doi:10.1017/S0022112090001914.

[16]   D. Saintillan and M. J. Shelley, "Active suspensions and their nonlinear models", *C. R. Physique* **14** (2013) 497–517; doi:10.1016/j.crhy.2013.04.001.

[17]   R. V. Vincent and N. A. Hill, "Bioconvection in a suspension of phototactic algae", *J. Fluid Mech.* **327** (1996) 343–371; doi:10.1017/S0022112096008579.

[18]   C. R. Williams and M. A. Bees, "Photo-gyrotactic bioconvection", *J. Fluid Mech.* **678** (2011) 41–86; doi:10.1017/jfm.2011.100.

[19]   H. Wioland, E. Lushi and R. E. Goldstein, "Directed collective motion of bacteria under channel confinement", *New. J. Phys.* **18** (2016) 075002; doi:10.1088/1367-2630/18/7/075002.

[20]   Z. Zhang, J. Liu, J. Meriano, C. Ru, S. Xie, J. Luo and Y. Sun, "Human sperm rheotaxis: a passive physical process", *Natur. Sci. Rep.* **6** (2016) 23553; doi:10.1038/srep23553.